

Article

A High-Reliable Wireless Sensor Network Coverage Scheme in Substations for the Power Internet of Things

Yiteng Lin, Tao Zhou *  and Zekai Wang

Institute of Broadband Wireless Mobile Communications, Beijing Jiaotong University, Beijing 100044, China

* Correspondence: taozhou@bjtu.edu.cn

Abstract: With the construction of the Power Internet of Things (PIoT) in full swing as well as the development of wireless communication technology, the deployment of wireless sensor networks is the key to the intelligent transformation of power systems. This paper proposes an asymmetric double-layer wireless sensor network coverage scheme for the intelligent substation. We conducted field measurements in the substation to record the received power at different locations, which were compared with the prediction results of the simulation model established by Winprop to verify the effectiveness of the simulation method. Based on the simulation platform, two different simulation models of substation scenarios are built, including a 220 kV outdoor substation and a 110 kV GIS room. The coverage of received power and line-of-sight (LOS) transmission are analyzed for various nodes of different layers. Several node distribution planning methods are proposed and proven to be feasible according to the simulation results. The wireless coverage scheme can provide useful references for the implementation of PIoT in substations.

Keywords: power internet of things (PIoT); intelligent substation; wireless sensor network; node distribution planning



Citation: Lin, Y.; Zhou, T.; Wang, Z. A High-Reliable Wireless Sensor Network Coverage Scheme in Substations for the Power Internet of Things. *Symmetry* **2023**, *15*, 1020. <https://doi.org/10.3390/sym15051020>

Academic Editors: Angelo Freni and Christos Volos

Received: 31 March 2023

Revised: 14 April 2023

Accepted: 1 May 2023

Published: 4 May 2023



Copyright: © 2023 by the authors. Licensee MDPI, Basel, Switzerland. This article is an open access article distributed under the terms and conditions of the Creative Commons Attribution (CC BY) license (<https://creativecommons.org/licenses/by/4.0/>).

1. Introduction

In recent years, the Power Internet of Things (PIoT) has attracted more and more attention because of its many potential benefits to power systems [1]. The PIoT makes full use of wireless communication, artificial intelligence (AI), and other technologies to facilitate interconnection and communication between facilities in the power system so as to accomplish real-time control and scientific decision-making. There are various new services derived by the PIoT, such as substation inspection robots, power transmission and transformation status monitoring, precise load control, etc., which greatly reduce the time-consuming and troublesome manual operation and maintenance monitoring [2,3]. These improvements enable PIoT to be applied to distinct segments of the power grid, such as power generation, transmission, transformation, distribution, and consumption [4–7].

Compared to distribution and consumption, the transformation segment (e.g., substations) has attracted much less attention from the PIoT application perspective due to its difficult physical access and its extremely harsh environment. However, as an important intermediate segment, the information transmission of the substations heavily relies on wireless communication networks. It is vital to have in-depth knowledge of the radio propagation of the working environment [8]. Notably, the metal equipment such as transformers, GIS switches, bus bars, and towers in substations can seriously affect the transmission path of radio waves, and this multi-metal environmental characteristic causes typical reflections and scattering, resulting in severe losses and time delays [9–11]. Therefore, the deployment of PIoT in substation scenarios is quite challenging.

Advanced communication and network technologies are the key to building PIoT [12]. Some wireless communication technologies, such as ZigBee, wireless local area networks (WLANs), WiMAX, and low-power wide area networks (LPWANs), have been applied to

the implementation of PIoT [13–15]. By utilizing these technologies wisely, the wireless network can be tailored to the needs of the substation scenario, including communication rate, transmission distance, network structure, number of access points, etc. In [16], the disadvantages of conventional substation temperature measurement methods are analyzed, and the reliability of the system is verified by applying ZigBee technology to the substation for comparison. The author in [17] formed a wireless sensor network with battery-limited sensor nodes for monitoring, which substantially decreased the energy consumption of the sensor nodes. Although some communication technologies are proven to be applicable, a low-power consumption and high-flexibility wireless networking scheme is still missing in substations.

It is generally known that the sensor layer, i.e., the wireless sensor network, is an important component of PIoT architecture [18–20]. The wireless sensor network deploys a large number of nodes covering the target area or electrical installations; thus, a reliable network coverage scheme is the key to ensuring the safe and stable operation of substations. The author in [21] evaluates the importance of the nodes based on the communication topology layer and the power grid layer in the substation. In [22], a construction scheme for a wireless sensor network for intelligent substations is proposed based on electromagnetic radiation interference protection technology. In [23], a low-cost wireless sensor network is introduced to realize real-time monitoring and the location of local discharge sources by receiving signal strength. In [24], the author built a power IoT sensor network with a hierarchical deployment of communication technology and node collaborative networking. However, there is still a lack of evaluation of the coverage performance of wireless sensor network solutions.

To fill the aforementioned research gaps, this paper aims to investigate the wireless network coverage scheme for PIoT substation scenarios. The major contributions and novelties of this paper are as follows:

(1) A double-layer wireless network coverage scheme is proposed to support data transmission from different types of nodes, including data aggregation from short-range low-rate wireless sensor nodes and data upload from long-range high-rate sink nodes and high-bandwidth nodes;

(2) The simulation software Winprop is used to evaluate the coverage scheme, which enables scenario modeling and electromagnetic simulation. By comparing the measurement results of the field 110 kV GIS substation with the prediction results of the simulation model built based on the actual scenario, the simulation scheme is verified to be accurate and feasible;

(3) We simulated and analyzed the application results of the double-layer wireless network coverage scheme for two different substation scenarios and conducted coverage range analysis based on the potential deployment positions of different types of nodes, verifying the feasibility of this scheme.

(4) Based on the simulation results, several node planning suggestions are given, and corresponding simulation analyses are carried out to prove their effectiveness.

The rest of this paper is outlined as follows: Section 2 introduces the proposed double-layer wireless sensor network coverage scheme. Section 3 verifies the feasibility of simulation analysis for the coverage scheme. Then, the performance of the proposed wireless coverage scheme is evaluated, and node planning methods are given in Section 4. Finally, conclusions are drawn in Section 5.

2. Substation Double-Layer Wireless Coverage Scheme

A substation wireless sensor network is mainly composed of wireless sensor nodes, high-bandwidth nodes, sink nodes, and access nodes. The operation of a wireless sensor network requires coordination between different types of nodes. Firstly, the wireless sensor nodes sense the environment and device states, which are translated into data and sent to the sink nodes. Based on the practical environment monitoring requirements, various sensors are installed for different substation scenarios, for example, temperature and humidity

sensors in the switch room and SF6 sensors in the GIS room. Subsequently, multiple types of sensing data are centrally transmitted to the access nodes by sink nodes after proper processing. Finally, the access nodes aggregate the data within the communication range, perform edge computing, and then remotely upload the data to the base station through an APN or 4G private network.

Concerning the deployment of the wireless network in the substation, it is vital to take into account the universality of the wireless network coverage scheme for different monitoring equipment, substations of different levels, and different areas of substations of the same level. According to the field investigation and service demand analysis of the substation, we proposed an asymmetric double-layer wireless network coverage scheme, which is shown in Figure 1. This scheme divides the wireless network into two layers based on the size of the transmitted data. In the first layer, the wireless transmission targets sensing terminals with small sizes, low power consumption, and high security. The terminals include micro-power sensor nodes and low-power consumption sensor nodes, which are covered by sink nodes adopting short-range communication technology. The former transmits high-frequency, small-data-volume (below KB-level) sensing information with μ W-level transmission power, while the latter transmits relatively large amounts of data with mW-level power. The second layer establishes wireless transmission links with a data volume of MB-level between access nodes and sink nodes, mobile high-bandwidth nodes, and fixed high-bandwidth nodes. The links operate in the power wireless private network to ensure high transmission rates and distances. With different transmission links for different orders of magnitude of data, the hierarchical coverage scheme can effectively improve bandwidth utilization and reduce energy consumption.

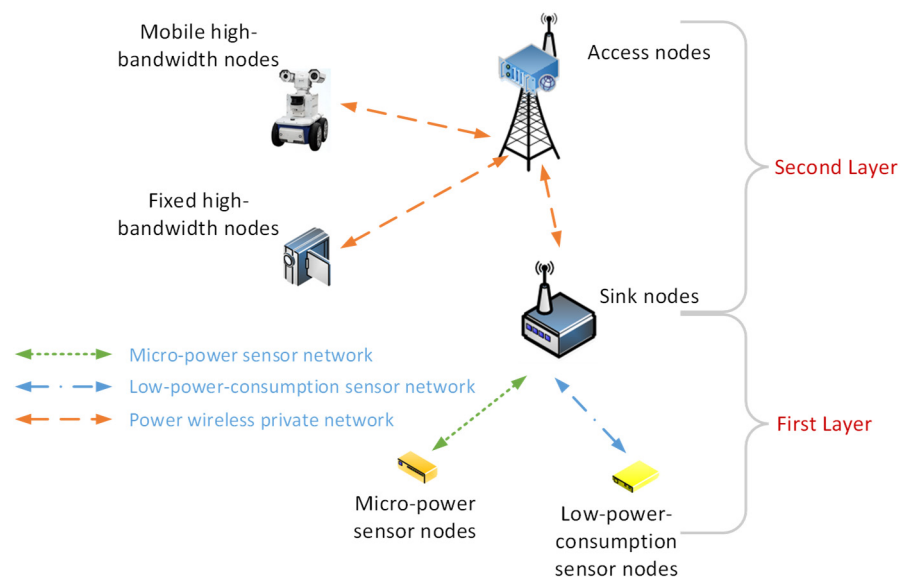


Figure 1. Schematic diagram of double-layer wireless network coverage.

3. Reliability Analysis of the Wireless Coverage Scheme

Since the large-scale deployment of wireless sensor networks in substations is an engineering problem that requires careful action, it is necessary to evaluate the feasibility of a coverage scheme based on simulation experiments. It seems to be a feasible method to build simulation models based on the actual substation environment to simulate the propagation of radio waves. To confirm that the simulation models are accurate and reliable, we carried out field measurements at the substation and compared the measurements with the simulation results for verification.

3.1. Measurement Campaigns

Taking into account the voltage level of the substation and the generality of the measurement scenario, a 110 kV GIS substation in Fengtai District, Beijing, is selected for field measurements and a wireless network coverage investigation. The 110 kV GIS substation has a 9.4 m length and 6.6 m width, and its internal structure is shown in Figure 2. It can be seen that its center is a large substation facility, surrounded by various metal equipment and sensor devices. We focus on the deployment of wireless sensor nodes, sink nodes, and access nodes in substation scenarios and the trajectory of mobile high-bandwidth nodes. In addition, the complex metal installations in the substation, such as transformers, GIS switches, busbars, towers, etc., are also investigated, which can complicate the electromagnetic propagation characteristics in substations.



Figure 2. Internal structure of the 110 kV GIS substation.

Figure 3 shows various sensors and sink nodes installed in the GIS substation, including a transformer core grounding current sensor, an ultrasonic partial discharge sensor, a variable frequency partial discharge sensor, and sink nodes. Different types of sensor nodes are deployed in the target work area, such as the surface of the device, the wall of the substation, etc. Since the location of the sensing nodes is usually fixed, the aggregation nodes need to be deployed in a reasonable location to reduce the impact of the surrounding environment.

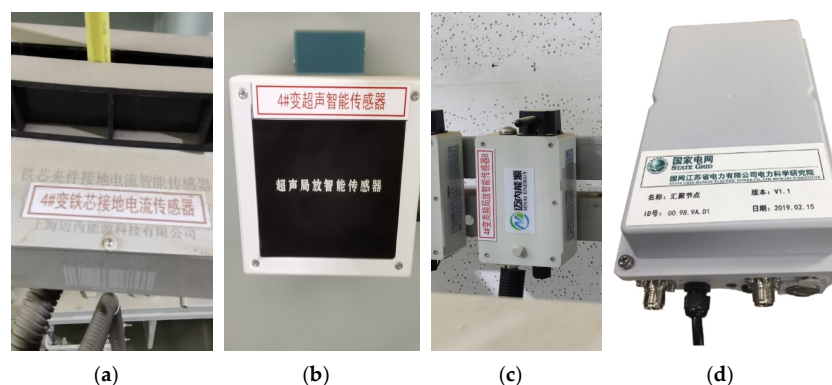


Figure 3. The sensor nodes and sink nodes deployed in the GIS substation are: (a) transformer core grounding current sensor; (b) ultrasonic partial discharge sensor; (c) variable frequency partial discharge sensor; and (d) sink nodes.

The main measurement work is oriented toward the radio wave propagation characteristics in the complex electromagnetic environment of the substation. Hence, a channel

sounder is designed to perform radio wave propagation measurements for substation scenarios, as shown in Figure 4.

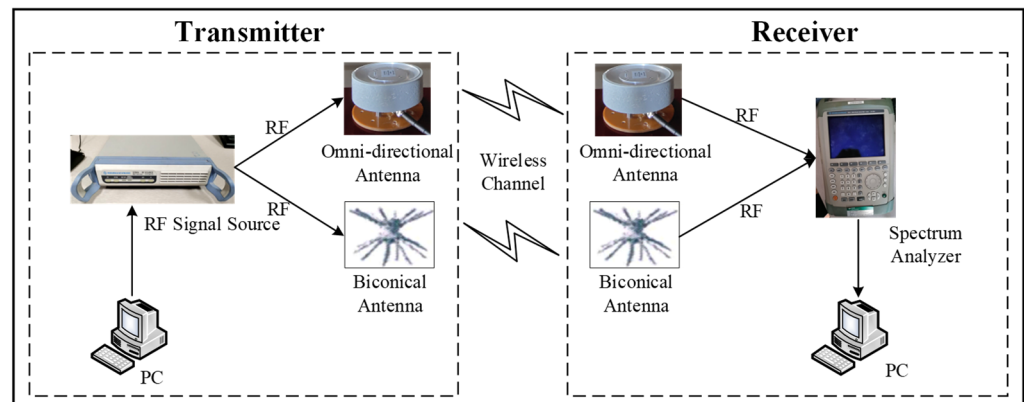


Figure 4. Measurement system architecture.

The transmitter (TX) is composed of an R&S SGS 100A RF signal source, a PC, and transmit antennas. The receiver (RX) consists of an R&S FSH4 handheld spectrum analyzer, a PC, and receive antennas. The spectrum analyzer supports a frequency band of 9 kHz–3.6 GHz, and the resolution bandwidth (RBW) is 1 Hz, which is convenient for obtaining real-time information. To support different frequency bands, different types of antennas are used, including omnidirectional antennas and biconical antennas. The frequency range of an omnidirectional antenna is 2 GHz–18 GHz, while the biconical antenna works at 500 MHz–3000 MHz. The basic working process of the channel sounder is as follows. On the TX side, the RF signal source is configured by the control software SGMA-GUI of the upper computer and generates the RF signal, which is transmitted through the cable and TX antenna. On the RX side, the fading RF signal is received by the RX antenna and transmitted to the spectrograph through the RF line. Then perform the data acquisition and storage according to the measurement needs.

Based on the field survey of the 110 kV GIS substation, the substation arrangement and corresponding planned measurement scheme are shown in Figure 5. The measurement route is counterclockwise around the central facility from the lower left corner, which refers to the inspection trajectory of mobile high-bandwidth nodes. The TX is fixed, and the RX moves along the measurement route at an interval of 1 m and collects data for a total of 24 positions. The TX antenna is 2.5 m in height, and the transmitting frequency and power are 2400 MHz and 10 dBm, respectively. In addition, the detection signal is set as a single-tone signal.

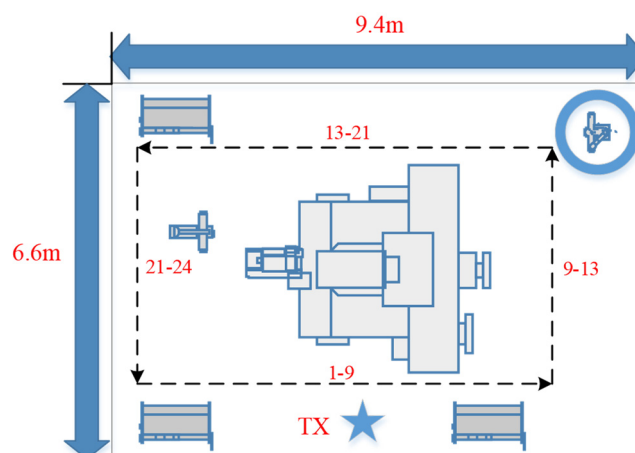


Figure 5. Substation arrangement and measurement route.

3.2. Simulation Model

Winprop is a comprehensive simulation tool that supports wireless propagation and radio network planning, allowing not only the modeling of simulation scenarios but also the deployment of antennas to predict wireless propagation. There are several simulation methods that can be chosen for radio propagation prediction, for example, empirical models, semi-empirical models, and ray optical propagation models. We built a 3D model of the 110 kV GIS substation with the components provided by Winprop, as shown in Figure 6a. The model is made regarding the actual substation scenario in terms of size and material. It is essential to choose a rational propagation model according to the characteristics of the environment. In most typical propagation scenarios, a dominant propagation path contributes more than 90% of the total energy. Although the substation is a multipath-rich environment, it is still dominated by LOS communications. Hence, the dominant path model (DPM) was used to build the simulation model based on a trade-off between complexity and accuracy. Since the DPM does not require pre-processing of the building vector database, it is well-suited for large indoor areas. Figure 6b shows the plan view of the simulation model in which the transmission antenna is placed at site 1. The configuration of the transmitter is fully referenced to the actual measurement.

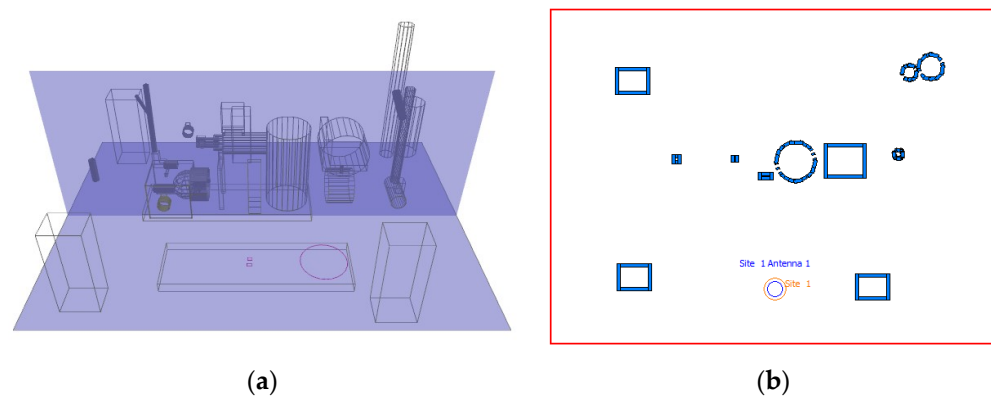


Figure 6. Simulation model of the 110 kV GIS substation. (a) The 3D simulation model; (b) the antenna layout.

The DPM determines the primary path between the transmitter and each receiver node. The path loss is calculated as

$$L = 20 \log\left(\frac{4\pi}{\lambda}\right) + 10p \log(l) + \sum_{i=1}^n f(\phi, i) + \sum_{j=1}^m t_j - \Omega \quad (1)$$

where l donates the distance between TX and RX, p represents the PL exponent that is relevant to the propagation environment, λ is wavelength, f represents the interaction loss caused by diffraction that accumulates along the propagation path, t means the loss of transmission. Since the reflection and scattering losses are not negligible, an empirically determined waveguide factor Ω is introduced. Given that the electromagnetic waves propagating in the corridor are less attenuated after reflection from the walls compared to free space, the waveguide effect can be expressed as an additional gain in decibels (dB). By applying the DPM for propagation forecast, a series of simulation parameters can be obtained, such as global received power, ray path diagram, path loss diagram, etc.

3.3. Comparative Analysis of Measurement and Simulation Results

Figure 7 depicts a comparison of the received power between the measured and simulated results. On the whole, it can be seen that the magnitude and variation trend of the received power between the simulation and measurement are consistent. In terms of sub-segments, the received power at reception points 1–9 shows a trend of increasing

and then decreasing, where the propagation condition between TX and RX is LOS. The overall received power is larger because it is not affected by obstacles, and the strongest received power is at the 5th receiving point closest to the TX antenna. Since the direct path is blocked by the equipment, the received power at reception points 9–13 shows a decreasing trend with the movement. The reception points 13–21 are completely in the non-line-of-sight (NLOS) condition, which results in a lower received power. Predictably, reception points 21–24 show the opposite trend to 9–13, and the result is exactly that. The comparison results show that the error of the simulation model is acceptable. Therefore, it is feasible to design and verify the wireless network coverage scheme through simulation.

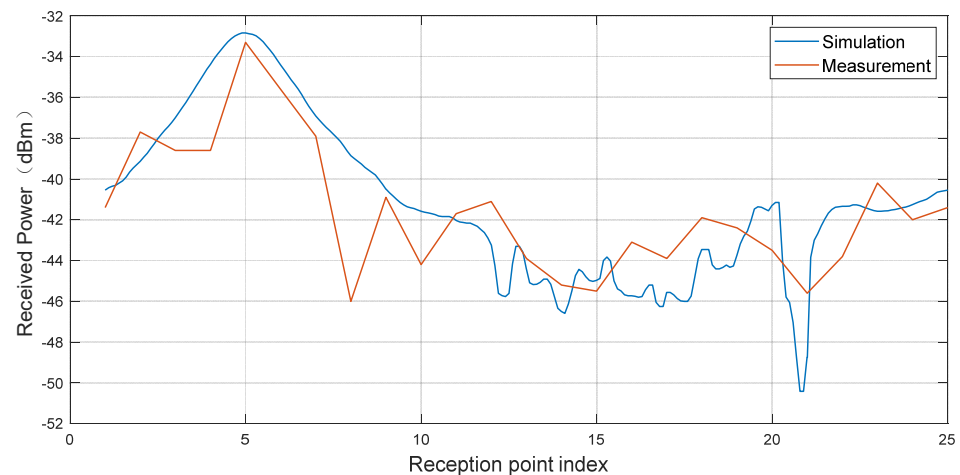


Figure 7. Comparison of received power between measured and simulated results.

4. Substation Wireless Sensor Network Coverage Simulation

4.1. Simulation of Wireless Coverage Scheme

Since the simulation model has been verified to be reliable, simulations are carried out for the double-layer wireless sensor network coverage scheme. For the first layer, the main simulation target is the power coverage of wireless sensor nodes, including the micro-power sensor nodes and low-power-consumption sensor nodes. With regard to the second layer, the distribution of received power for the sink nodes is generated and analyzed. It is noted that two typical indoor and outdoor substation scenarios are modeled to evaluate the coverage scheme comprehensively. These two substations are prototyped as an outdoor substation at 220 kV in Jiaying, Zhejiang, and a 110 kV GIS room in Jinhua, Zhejiang.

4.1.1. 220 kV Outdoor Substation

Figure 8 shows the simulation model and antenna layout diagram of the outdoor substation model established by Winprop. The specific environmental features and measurement configurations are as follows: The outdoor substation is 150 m in length and 100 m in width. There are two main transformers located in the middle of the substation, which are modeled as two huge rectangular metal obstructions. As for the material parameters, the relative dielectric constants of the concrete wall and floor are set to 5.31 and 3.66, respectively. The conductivity of concrete walls, floors, and metal cabinets is configured as 0.09 S/m, 0.02 S/m, and 9.9×10^6 S/m, respectively. According to the standardized communication protocol of the Internet of Things for transformer equipment, the 2.4 GHz frequency band was adopted in the simulation experiment. The transmitted power of micro-power sensor nodes, low-power consumption sensor nodes, and sink nodes is set to -10 dBm, 10 dBm, and 43 dBm, respectively. The deployment positions of the TX antennas are shown in Figure 8b, which are placed at sites 1 and 3, with a height of 2.5 m. Generally speaking, the receiving sensitivity of sink nodes is between -90 dBm and -129 dBm. To make the results universal, the maximum value of this range is determined as the threshold, and the area where the received power is below -90 dBm is regarded as the coverage

blind area. Based on the above settings, the power coverage of the two layers is simulated and analyzed.

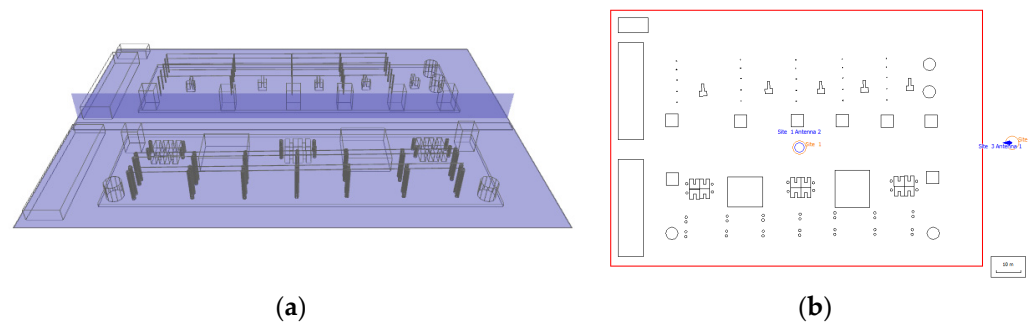


Figure 8. Simulation model of a 220 kV outdoor substation: (a) 3D simulation model; (b) antenna layout.

We first analyze the low-power consumption sensor nodes in the first layer coverage of the 220 kV outdoor substation, and the wireless coverage prediction results with the TX antenna on site 1 are shown in Figure 9.

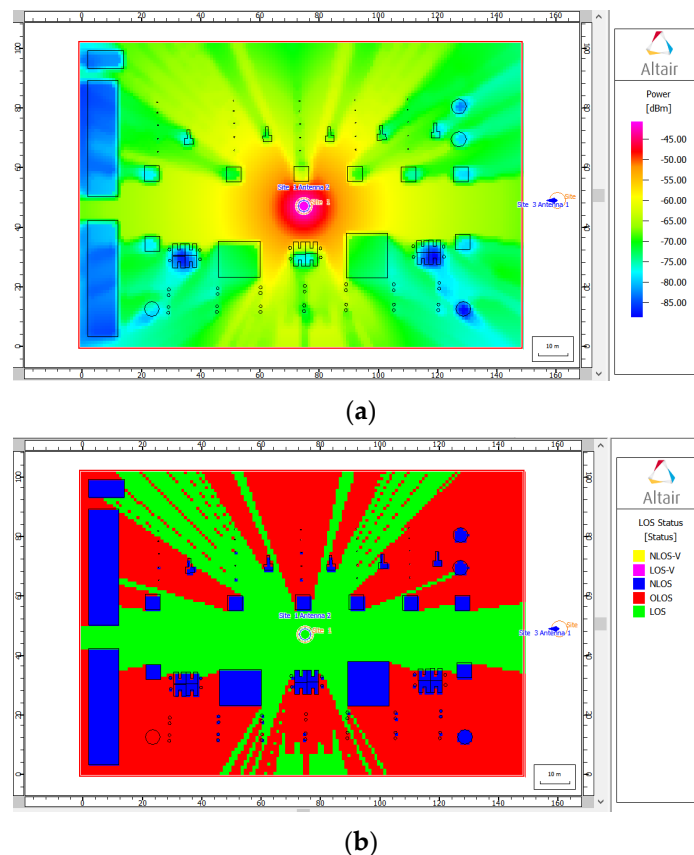


Figure 9. Wireless coverage prediction for low-power consumption sensor nodes in a 220 kV outdoor substation. (a) Distribution diagram of received power; (b) distribution of LOS transmission.

In Figure 9a, the received power of the low-power-consumption nodes is higher than the threshold from an overall perspective, which implies excellent wireless coverage performance. Due to the blockage of metal equipment, there is significant fading of received power behind the obstacles, forming a deep fading area. It can be seen in Figure 9b that the distribution of LOS transmission is in the open corridor area, metal equipment gap, and part rear areas. While most areas behind the metal equipment are in obstructed line-of-sight (OLOS) communication because the radio waves are diffracted when encountering

electrical equipment. Note that the electrical equipment experienced NLOS transmission due to higher transmitting antennas or metal enclosures with electromagnetic shielding.

In the actual deployment of wireless networks, the Zigbee transmission protocol is usually used in substations, and the sensitivity of receivers based on this protocol is usually -97 dBm. Since there is a certain amount of electromagnetic noise in the actual environment of substations, the use of -90 dBm as the sensitivity of the sink node in this paper can provide sufficient fading margin to avoid the lack of reference meaning provided by this result. If it is in the less complex scenario of electrical equipment distribution, the network coverage using the Zigbee transmission protocol can be somewhat extended in the simulation results.

Figure 10a,b illustrates the diagrams of received power and LOS transmission of micro-power sensor nodes. Notably, there are obvious coverage blind areas behind the metal obstacles and at the corners of the substation, which are caused by lower transmitted power. Therefore, it is necessary to plan the micro-power sensor nodes and sink nodes reasonably. Furthermore, the result of LOS transmission is almost the same with low-power consumption sensor nodes.

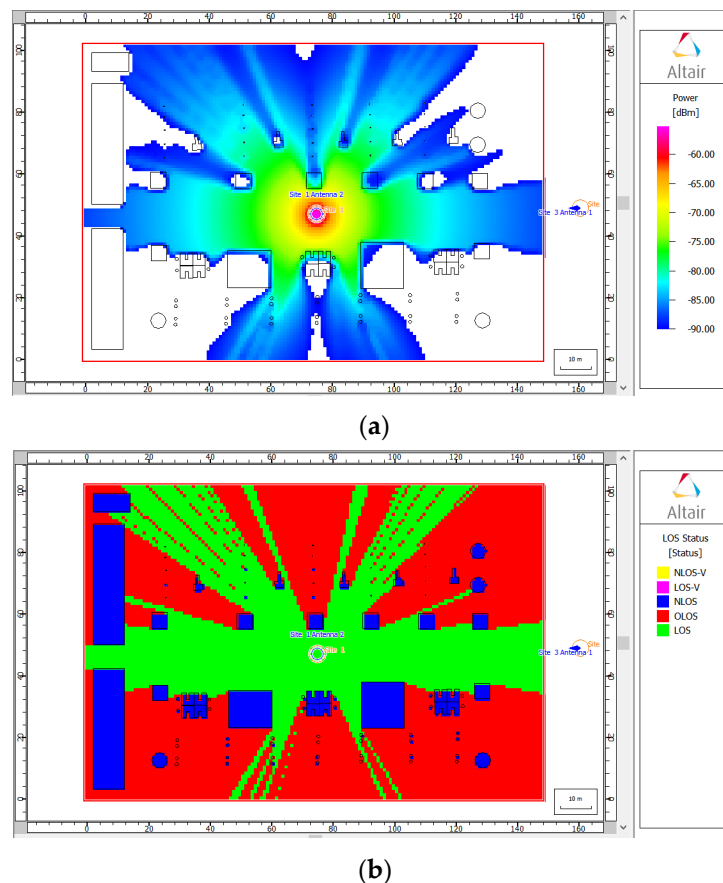


Figure 10. Wireless coverage prediction for micro-power sensor nodes in a 220 kV outdoor substation. (a) Distribution diagram of received power; (b) distribution of LOS transmission.

Then, the coverage situation of the second layer is forecasted based on the TX antenna located on site 3, which is shown in Figure 11. In Figure 11a, the received power can achieve full coverage of the substation. From Figure 11b, it can be seen that the main corridor where the sink nodes and mobile high-bandwidth nodes are located is in LOS transmission. And some fixed high-bandwidth nodes are located behind the metal facilities, which are in OLOS transmission, but they can still meet the basic requirements of wireless coverage.

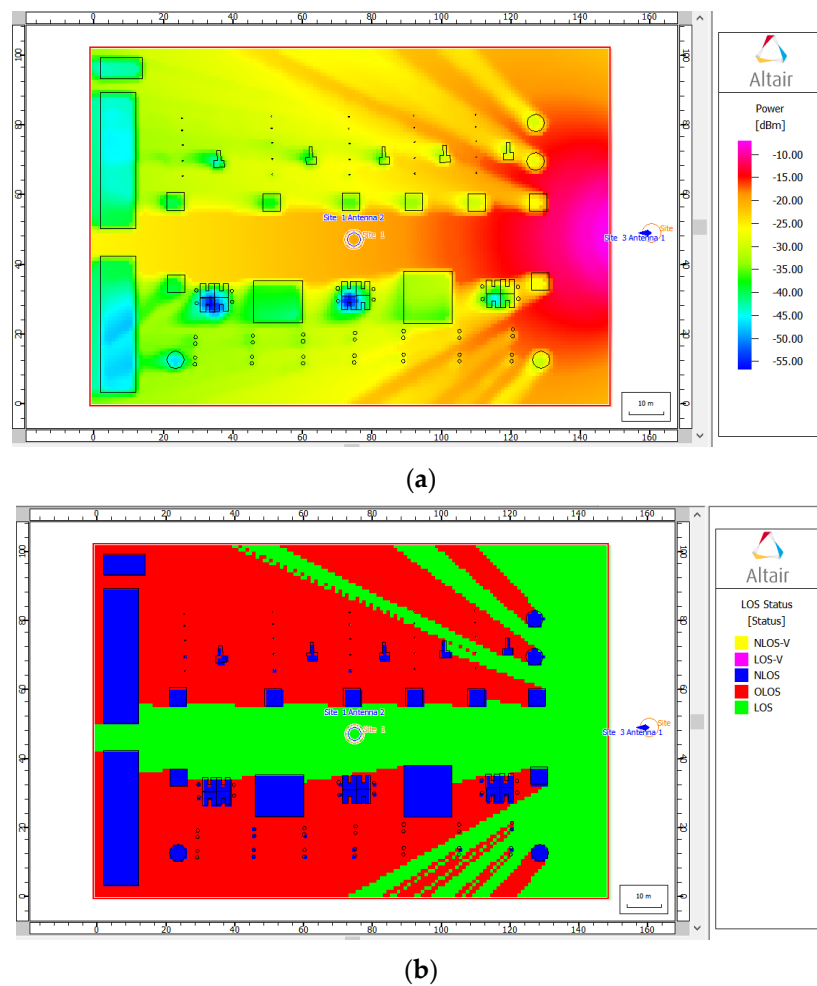


Figure 11. Wireless coverage prediction for sink nodes in a 220 kV outdoor substation. (a) Distribution diagram of received power; (b) distribution of LOS transmission.

4.1.2. 110 kV Indoor Substation

The simulation model and antenna layout of the 110 kV GIS room are built in the same way and are shown in Figure 12. The GIS room is 30 m in length and 20 m in width, which is larger than that in Section 3. Various equipment like circuit breakers, bus bars, isolators, etc. is modeled as structures with different shapes. These modules are centrally located in the middle of the room, which will have a significant impact on radio propagation. The material parameters and setup of transmitters are the same as those in the outdoor substation.

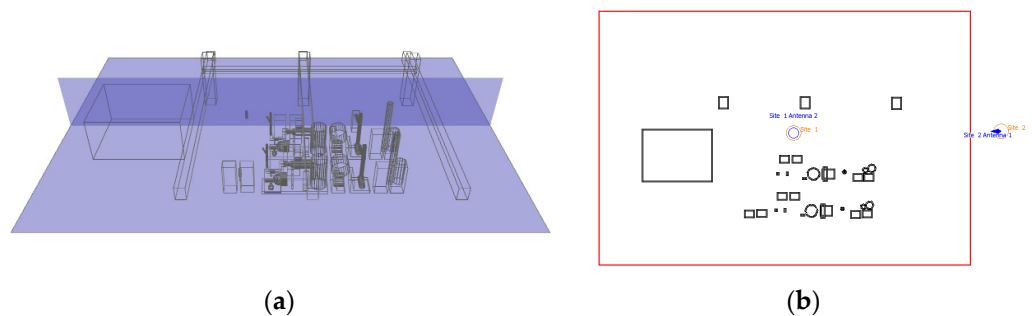


Figure 12. Simulation model of a 110 kV GIS room. (a) The 3D simulation model; (b) the antenna layout.

Similarly, the received power coverage of the first layer of the wireless sensor network is simulated and calculated first with the transmitter at site 1. In Figure 13, the wireless

coverage prediction results of low-power consumption nodes are plotted, including the diagram of received power and LOS transmission. Due to the small area, the received power at any position in the GIS room meets the requirements of receiving sensitivity. From Figure 13b, most areas are in LOS and OLOS communication, while the metal equipment shells and pipes are in NLOS.

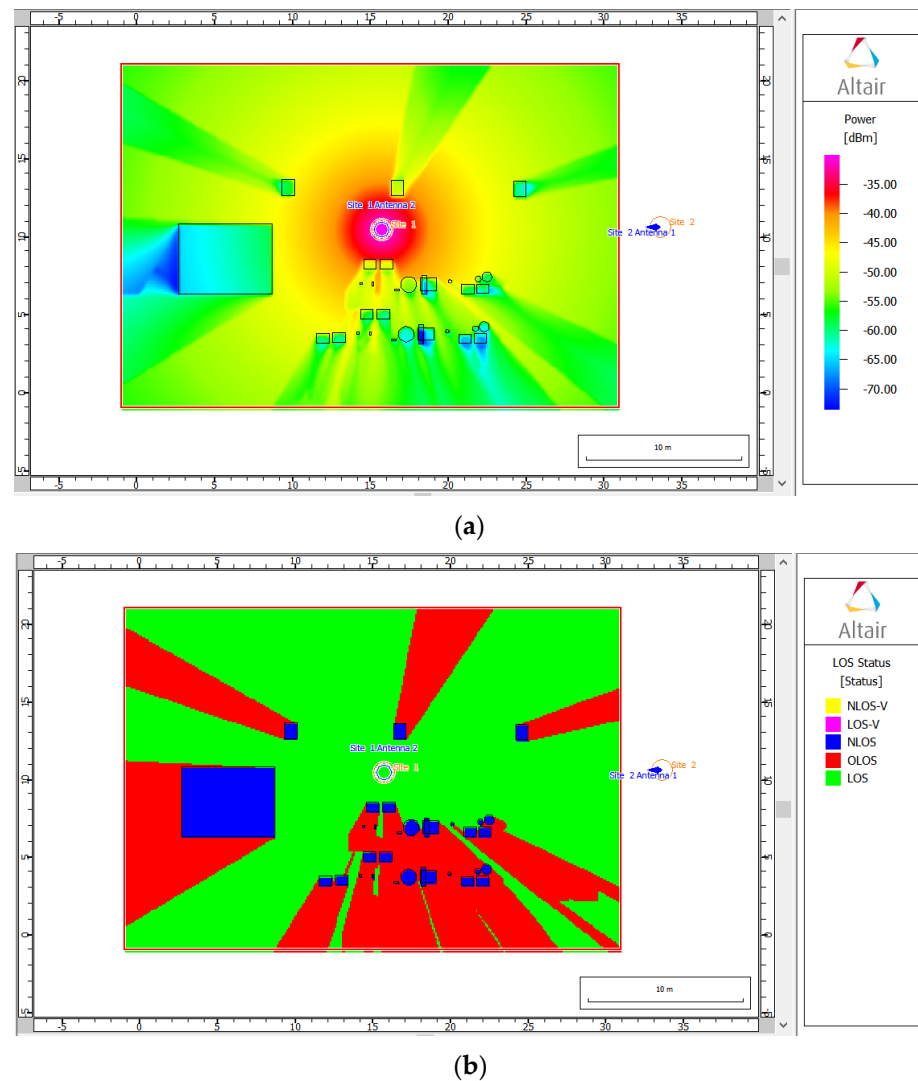


Figure 13. Wireless coverage prediction for low-power consumption sensor nodes in a 110 kV GIS room. (a) Distribution diagram of received power; (b) distribution of LOS transmission.

Figure 14 shows the simulation results of the received power and LOS transmission of micro-power sensor nodes in the 110 kV GIS room. Although the transmitted power is lower, the receiving power can cover of almost the whole indoor scenario. Since LOS transmission mainly depends on the arrangement of the substation and location of the TX antenna, which leads to the same LOS transmission results.

Figure 15 illustrates the simulation results of sink nodes in the 110 kV GIS room. It can be seen that the TX antenna located in site 2 can achieve full coverage of the indoor substation with a higher received power. The sink nodes and high-bandwidth nodes can be covered by LOS or OLOS transmission, which meet the basic requirements of wireless coverage.

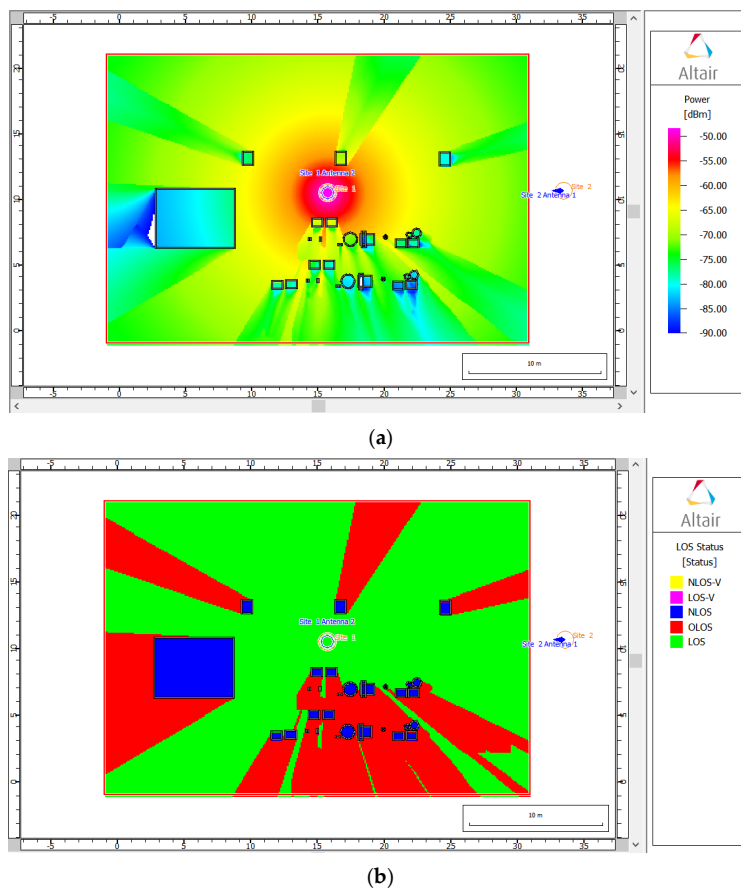


Figure 14. Wireless coverage prediction for micro–power sensor nodes in a 110 kV GIS room. (a) Distribution diagram of received power; (b) distribution of LOS transmission.

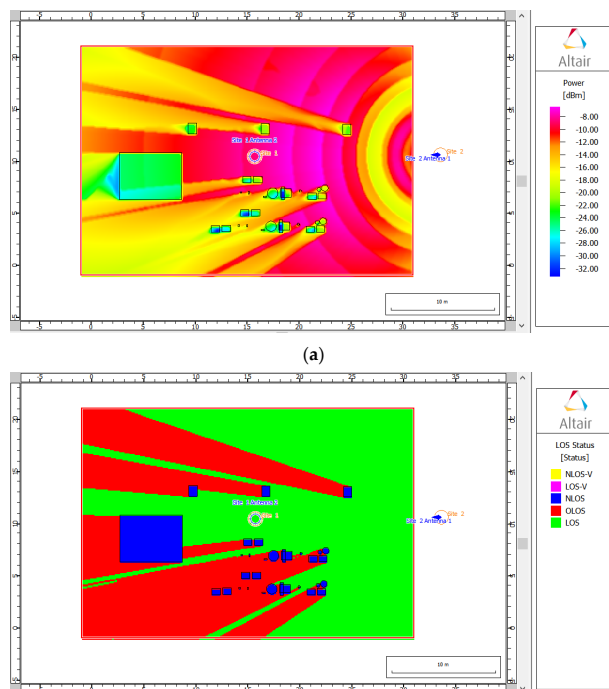


Figure 15. Wireless coverage prediction for sink nodes in a 110 kV GIS room. (a) Distribution diagram of received power; (b) distribution of LOS transmission.

In summary, through the deployment of potential locations of sink nodes and access nodes in the proposed wireless two-layer coverage network, the signal attenuation of different transmission layers and the coverage of the wireless network in specific scenarios are obtained, thus verifying that the new wireless network architecture has certain rationality and can better realize the network coverage of indoor and outdoor substations. In addition, the sensing devices can be deployed in practice based on the simulation results as a reference to avoid deployment in coverage-blind areas.

4.2. Node Planning for Wireless Sensor Network

The simulation results described in the last subsection reveal some deficiencies in the coverage performance of the double-layer wireless sensor network. Therefore, it is vital to adopt some targeted improvements, for instance, in the planning of nodes. It can be found that low-power-consumption sensor nodes and sink nodes achieve better coverage performance in both indoor and outdoor scenarios. In contrast, the micro-power sensor nodes have a large number of coverage-blind areas in outdoor substations due to power limitations. Additionally, there are large areas where the received power is close to the threshold, i.e., the area indicated with dark blue in the diagrams of received power. Theoretically, the reception sensitivity can be achieved at the sink nodes, but it is difficult to ensure the reliability of data transmission at this layer considering the fading margin problems caused by environmental factors, weather, etc. Therefore, optimization of wireless coverage for micro-power sensor nodes is needed, especially in the outdoor substation.

There are two major optimization strategies proposed for the micro-power sensor nodes. The first is to increase the number of sink nodes and reasonably deploy them in blind areas. After investigation, a standard substation usually requires 5–10 sink nodes to achieve wireless coverage of the whole station. Meanwhile, the cost should be considered to provide reliable coverage of all sensor nodes with as few sink nodes as possible. Obviously, a sink node has limited coverage capacity for micro-power nodes, so we placed a sink node at each of the four corners of an outdoor substation with a significant blind area. Figure 16 shows the coverage diagrams of received power for the four sink nodes. It can be observed that most of the areas in the substation have reached the wireless coverage requirements after the addition of new sink nodes. Some individual receiving nodes that do not meet the requirements appear in the gap between the substation box and the wall, the safety work box, and the interior of some substation boxes.

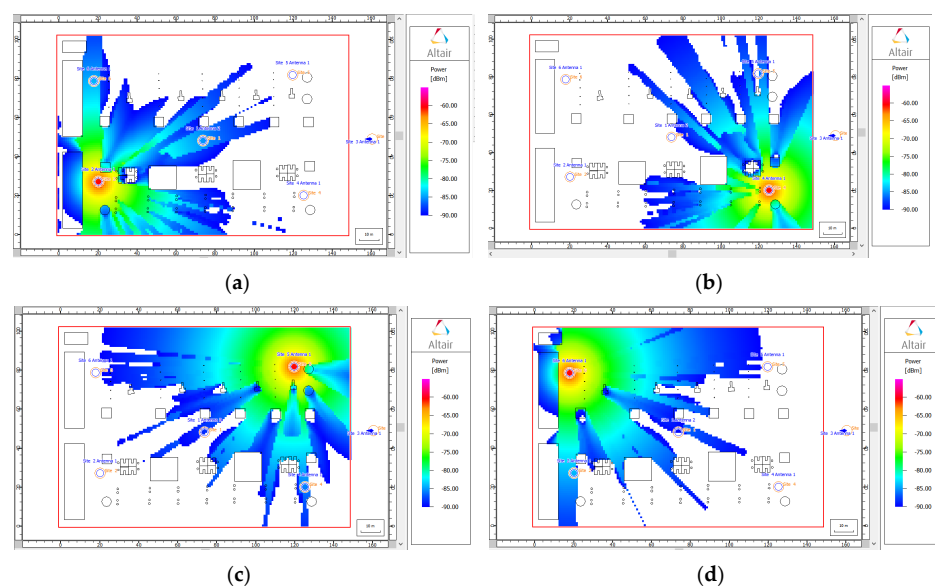


Figure 16. Coverage diagrams of received power for the added four sink nodes. (a) deployed in the bottom left corner; (b) deployed in the bottom right corner; (c) deployed in the upper right corner; (d) deployed in the upper left corner

Taking Figure 16b as an example, the received power variation of the propagation path from the sink node to the inside of the transformer is shown in Figure 17. It is visible that the received power inside the transformer box is between -90 dBm and -95 dBm due to the severe penetration loss, but the nodes around and on the surface of the transformer can be well covered. Hence, a reasonable increase and arrangement of the sink nodes can reduce the coverage blind area for micro-power sensor nodes, and at the same time, it can reduce the data transmission burden with only a single node.

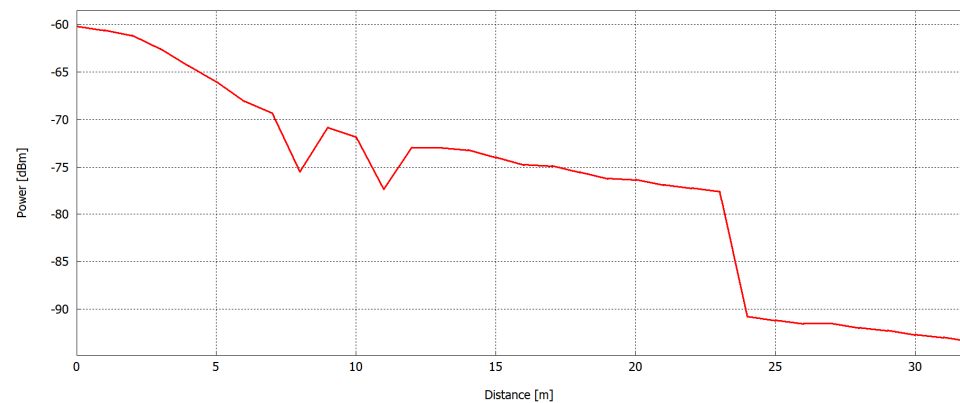


Figure 17. Received power from the sink node to the transformer.

The second strategy is to reduce the transmission frequency band of the micro-power sensor nodes, such as the 1.8 GHz frequency band, which is also supported by the power wireless network. A lower frequency band means lower path loss and better coverage. Furthermore, the micro-power sensor nodes require only low transmission rates, and the 1.8 GHz band can provide sufficient bandwidth. The coverage diagrams of received power in the 1.8 GHz frequency band are shown in Figure 18. It can be found that the areas that meet the coverage are increased, and the space between the transformer boxes and the rear area is well covered. In addition, owing to the small space between the substation box and the wall clearance and inside the safety work box, no wireless sensing nodes are usually arranged. Therefore, the second strategy can also effectively solve the wireless coverage problem of some nodes at the edge of the substation.

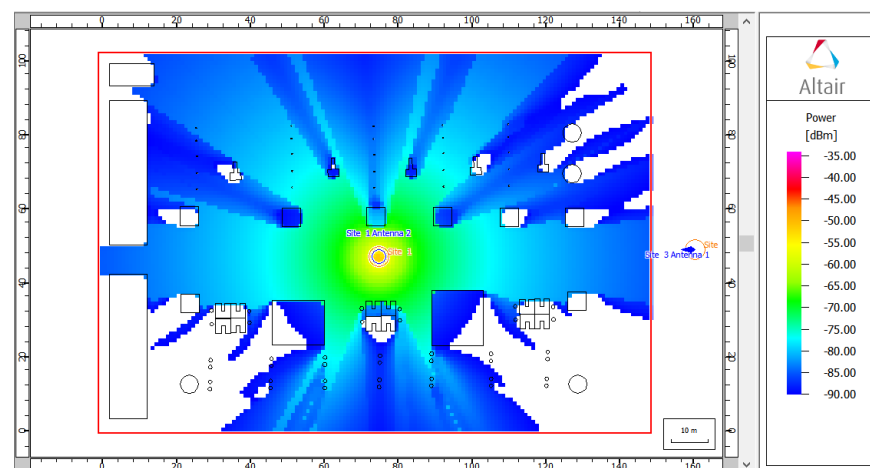


Figure 18. Coverage diagrams of received power for the second strategy.

In addition to the two specific optimization measures mentioned above, there are some other methods that can improve the coverage quality in combination with the scenario characteristics of the substation. For example, under the premise of meeting the business monitoring needs of smart substations and the monitoring quality of wireless sensors, LOS

transmission between wireless sensor nodes and sink nodes should be achieved as far as possible, which can reduce the impact caused by shadow fading and increase the wireless transmission distance.

5. Conclusions

In this paper, the wireless sensor network in an intelligent substation for PIIoT has been investigated. We have designed an asymmetric double-layer wireless coverage scheme that mainly contains sensor nodes, sink nodes, and access nodes. To evaluate the coverage scheme, the simulation software Winprop was used to model the substation scenarios and perform wave propagation predictions. Before that, the reliability of the simulation model had been verified. A measurement system has been designed and used for field measurement in a 110 kV GIS room, and then the received power at measurement points is compared with the simulation results at the same places, which show a similar magnitude and variation trend. Subsequently, a 220 kV outdoor substation and a 110 kV GIS room have been modeled, and the materials parameters and measurement setup have been configured according to the standard and actual environments. The simulation predicts the coverage of different nodes in the two layers, which include micro-power nodes and low-power consumption nodes in the first layer and sink nodes in the second layer. The diagrams of received power and LOS transmission have been shown and analyzed for these nodes of two substations. The results have indicated that micro-power nodes possess a large blind area caused by lower transmitted power. Finally, several node planning methods have been proposed to improve coverage. From the results, increasing the number of convergence nodes as well as reducing the communication frequency can effectively improve coverage. On the whole, the double-layer wireless sensor network coverage scheme can achieve coverage for the target area and provide useful references for the deployment of PIIoT in substations.

Author Contributions: Conceptualization, Y.L.; Methodology, T.Z.; Software, Y.L.; Validation, Z.W.; Investigation, T.Z.; Data curation, Z.W.; Writing—original draft, Y.L.; Writing—review & editing, T.Z. All authors have read and agreed to the published version of the manuscript.

Funding: This work was supported by the Science and Technology Project of State Grid Corporation of China (Research on Reliability Technologies for Transformer Substation Wireless Networks in Complex Electromagnetic Environments, 5500-202055070A-0-0-00).

Data Availability Statement: Data sharing not applicable.

Conflicts of Interest: The authors declare no conflict of interest.

References

1. Dib, L.D.M.B.A.; Fernandes, V.; de L, M.; Ribeiro, M.V. Hybrid PLC/wireless communication for smart grids and internet of things applications. *IEEE Internet Things* **2018**, *5*, 655–667. [[CrossRef](#)]
2. Teshager, B.G.; Minxiao, H.; Patrobers, S.; Khan, Z.W.; Tuan, L.K.; Shah, F.M. Direct power control strategy based variable speed pumped storage system for the reduction of the wind power fluctuation impact on the grid stability. In Proceedings of the 2018 IEEE 12th International Conference on Compatibility, Power Electronics and Power Engineering (CPE-POWERENG 2018), Doha, Qatar, 10–12 April 2018; pp. 1–6.
3. Ma, L.; Li, W.; Hou, Y.; Zhan, W.; Yang, R.; Jia, W.; Qiu, Y. Application of wireless communication technology in ubiquitous Power Internet of Things. In Proceedings of the 2020 IEEE 3rd International Conference on Computer and Communication Engineering Technology (CCET), Beijing, China, 14–16 August 2020; pp. 267–271.
4. Pagani, G.A.; Aiello, M. Generating realistic dynamic prices and services for the smart grid. *IEEE Syst. J.* **2015**, *9*, 191–198. [[CrossRef](#)]
5. Zhou, T.; Lin, Y.; Yang, Z.; Ai, B.; Liu, L. Radio Channel Measurements and Characterization in Substation Scenarios for Power Grid Internet of Things. *IEEE Internet Things J.* **2023**, *10*, 7691–7704. [[CrossRef](#)]
6. Tung, H.Y.; Tsang, K.F.; Chui, K.T.; Tung, H.C.; Chi, H.R.; Hancke, G.P.; Man, K.F. The generic design of a high-traffic advanced metering infrastructure using ZigBee. *IEEE Trans. Ind. Inf.* **2014**, *10*, 836–844. [[CrossRef](#)]
7. Wang, Q.; Wang, Y. Research on power Internet of Things architecture for smart grid demand. In Proceedings of the 2018 2nd IEEE Conference on Energy Internet and Energy System Integration (EI2), Beijing, China, 20–22 October 2018; pp. 1–9.

8. Zhou, T.; Zhang, H.; Ai, B.; Liu, L. Weighted score fusion based LSTM model for high-speed railway propagation scenario identification. *IEEE Trans. Intell. Transp. Syst.* **2022**, *23*, 23668–23679. [[CrossRef](#)]
9. Sandoval, R.M.; Garcia-Sanchez, A.; Molina-Garcia-Pardo, J.; Garcia-Sanchez, F.; Garcia-Haro, J. Radio-channel characterization of smart grid substations in the 2.4-GHz ISM band. *IEEE Trans. Wireless Commun.* **2017**, *16*, 1294–1307. [[CrossRef](#)]
10. Zhou, T.; Zhang, H.; Ai, B.; Xue, C.; Liu, L. Deep-learning-based spatial-temporal channel prediction for smart high-speed railway communication networks. *IEEE Trans. Wirel. Commun.* **2022**, *21*, 5333–5345. [[CrossRef](#)]
11. Gungor, V.C.; Lu, B.; Hancke, G.P. Opportunities and challenges of wireless sensor networks in smart grid. *IEEE Trans. Ind. Electron.* **2010**, *57*, 3557–3564. [[CrossRef](#)]
12. Zhou, T.; Tao, C.; Salous, S.; Liu, L. Measurements and analysis of angular characteristics and spatial correlation for high-speed railway channels. *IEEE Trans. Intell. Transp. Syst.* **2018**, *19*, 357–367. [[CrossRef](#)]
13. Li, Y.; Cheng, X.; Cao, Y.; Wang, D.; Yang, L. Smart choice for the smart grid: Narrowband Internet of Things (NB-IoT). *IEEE Internet Things J.* **2018**, *5*, 1505–1515. [[CrossRef](#)]
14. Chettri, L.; Bera, R. A comprehensive survey on Internet of Things (IoT) toward 5G wireless systems. *IEEE Internet Things J.* **2020**, *7*, 16–32. [[CrossRef](#)]
15. Bedi, G.; Venayagamoorthy, G.K.; Singh, R.; Brooks, R.R.; Wang, K. Review of Internet of Things (IoT) in electric power and energy systems. *IEEE Internet Things J.* **2018**, *5*, 847–870. [[CrossRef](#)]
16. Huang, X.; Li, X.; Wang, Y.; Fang, S. An online temperature monitoring system of substation based on Zigbee wireless network. In Proceedings of the 2011 International Conference on Electrical and Control Engineering, Yichang, China, 16–18 September 2011; pp. 992–995.
17. Yildiz, H.U.; Gungor, V.C.; Tavli, B. A hybrid energy harvesting framework for energy efficiency in wireless sensor networks based smart grid applications. In Proceedings of the 2018 17th Annual Mediterranean Ad Hoc Networking Workshop (Med-Hoc-Net), Capri, Italy, 20–22 June 2018; pp. 1–6.
18. Lin, C.; Xiang, K.; Du, Y.; Li, Y.; Lin, H. Research on the Energy Internet Under the Background of Ubiquitous Power Internet of Things. In Proceedings of the 2019 IEEE 3rd Conference on Energy Internet and Energy System Integration (EI2), Changsha, China, 8–10 November 2019; pp. 403–407.
19. Zhai, Z.; Jia, L.; Ma, Y.; Jing, W.; Zhang, Z. Research on Ubiquitous Power Internet of Things Architecture. In Proceedings of the 2019 IEEE 3rd Conference on Energy Internet and Energy System Integration (EI2), Changsha, China, 8–10 November 2019; pp. 435–439.
20. Zhang, Z.; Li, W.; Meng, H. Multimodal network structure design of power communication. In Proceedings of the 2022 IEEE 6th Information Technology and Mechatronics Engineering Conference (ITOEC), Chongqing, China, 4–6 March 2022; pp. 1197–1201.
21. Zhou, M.; Rui, L.; Qiu, X.; Xia, Z.; Li, B. Evaluation of the Node Importance in Power Grid Communication Network and Analysis of Node Risk. In Proceedings of the 2018 IEEE/IFIP Network Operations and Management Symposium, Taipei, Taiwan, 23–27 April 2018; pp. 1–5.
22. Zhang, J.; Lv, L.; Zhu, M.; Zhang, Q. Research on Intelligent Substation Wireless Sensor Network System Architecture Based on Internet of Things Technology. In Proceedings of the 2020 Prognostics and Health Management Conference (PHM-Besançon), Besançon, France, 4–7 May 2020; pp. 324–327.
23. Upton, D.W.; Saeed, B.I.; Khan, U.; Jaber, A.; Mohamed, H.; Mistry, K.; Malher, P.J.; Lazaridis, P.; Vieira, M.Q.; Atkinson, R.; et al. Wireless sensor network for radiometric detection and assessment of partial discharge in HV equipment. In Proceedings of the 2017 XXXIInd General Assembly and Scientific Symposium of the International Union of Radio Science (URSI GASS), Montreal, QC, Canada, 19–26 August 2017; pp. 1–4.
24. Chen, B.; Chen, L.; Tan, Y.; Kuang, X. Investigations on communication and management techniques for electric Internet of Things applications in smart grid. In Proceedings of the 2021 China International Conference on Electricity Distribution (CICED), Shanghai, China, 7–9 April 2021; pp. 515–518.

Disclaimer/Publisher’s Note: The statements, opinions and data contained in all publications are solely those of the individual author(s) and contributor(s) and not of MDPI and/or the editor(s). MDPI and/or the editor(s) disclaim responsibility for any injury to people or property resulting from any ideas, methods, instructions or products referred to in the content.